International Journal of Social Robotics
https://doi.org/10.1007/s12369-025-01327-1

Modelling Proxemic Zone Shapes from Analytic and Simulated Motion Strategies

Fanta Camara[1,2,3] · **Charles Fox**[2,3]

Received: 10 October 2024 / Revised: 21 July 2025 / Accepted: 10 September 2025

Abstract

Autonomous robots need to navigate around and negotiate for space with humans. Proxemics is the study of zones of personal and social space which humans experience around themselves and others, and use to control spatial interactions. By formalizing proxemic zones, autonomous robots may interact similarly. This study shows how proxemic zones may be generated by kinetics and trust, with the social zone being the critical space in which a human must trust another agent to avoid collision under their possible future motions. Previous studies have formalized these kinematics but have assumed that zones are circular in shape and found only their radii. However the kinematics and trust concepts used to generate them enable models to take account of the heading and rotational kinematics involved. This is shown to result in new non-circular shapes for the proxemic zones, whose egg shapes match those which have been found empirically and assumed without prior theory by current practical robots. Numerical and approximate analytical solutions to describe the zone shapes and sizes are presented. Zones are shown to change shape and size in response to the properties of the other agent, and are shown to generalize to include the stopping distances taught to drivers and pedestrians as well as natural human body zones.

Keywords Proxemics · Trust · Human-robot interaction

1 Introduction

Autonomous robots which operate around humans are becoming common in research, and claimed as commercial products. These include full-size self-driving cars and smaller last-mile delivery vehicles, as well as humanoid service robots, which must all share and negotiate for space with humans on roads, pavements, pedestrianized areas and indoors. The theory of these interactions is still not understood, and remains a key question in human-robot interaction (HRI).

Like most engineering systems, robots are traditionally designed with the objective of being as safe as possible. In cases of human interaction, this has included behaviours which stop or otherwise give way (yield) to humans in every case of possible collision. While this can lead to successful interactions in sparsely populated environments, it becomes a problem when there are higher densities of humans, such as large groups crossing roads in cities, and crowded human areas. In these cases, the robot may 'freeze', yielding forever to a continual stream of humans, and never making progress to its destination. This scenario has become known as the 'freezing robot problem' [1]. However, in human-human interactions, humans are well known to be able to resolve such conflicts. If only we had a better model of human-human interaction then it could be applied to HRI too.

The *sequential chicken* model, using game theory, has been proposed [2] as a solution to the freezing robot problem. Here, both agents plan to move towards each other, or to yield, based on their estimates of both the probability and their utilities of a collision occurring, versus the value of time lost by yielding. By both allowing and planning for a

✉ Fanta Camara
fanta.camara@york.ac.uk

Charles Fox
chfox@lincoln.ac.uk

[1] Institute for Safe Autonomy, University of York, York, UK

[2] Institute for Transport Studies, University of Leeds, Leeds, UK

[3] Lincoln Centre for Autonomous Systems, University of Lincoln, Lincoln, UK

Published online: 01 December 2025

small but strictly non-zero probability of a collision occurring, they can usually create a successful interaction.

The sequential chicken model creates good interactions most of the time, but at the cost of requiring occasional interactions to result in collision in order to provide a game theoretic credible threat. For human-human interactions such as pedestrians trying to avoid each other on a sidewalk, this may be considered acceptable, as pedestrians do occasionally touch one another, without causing serious damage or distress. However for interactions between humans and robots – especially large robots such as autonomous vehicles – collision could be dangerous and even fatal. The sequential chicken model's game theory can however be extended to remove the need for rare collisions if some weaker penalty can be found and inflicted more frequently.

Humans are known to have several discrete psychological spatial zones surrounding them, and to experience different types of discomfort if these zones are occupied without their consent [3]. The study of these zones is known as *proxemics*. Different types of people can enter different zones without causing discomfort. The proxemic zones are [3]: an intimate zone (for family) ranging up to 0.45 m from the human's center point; a personal zone (for friends) up to 1.2 m; a social zone (for business associates) up to 3.7 m, and a public zone (for speaking to strangers) up to 7.5 m. For example, social distancing measures during the COVID-19 pandemic pushed personal interactions out into the social zone, causing friends to be treated like business associates. It has been proposed in [4] that deliberate invasion of the social zone by other humans, or by robots, could be used with the chicken model as an improved interaction control, replacing the need for even rare collisions with more frequent but much smaller negative utilities incurred from space invasion, to enable the same quality of interaction but without ever risking serious harm. Early proxemics studies reported empirical results on zone sizes and utilities, but to use them for active interaction control in HRI, a generative, quantitative theory is needed. Rios-Martinez et al. [5] proposed a comprehensive review of proxemics for human-robot interactions and the authors hinted that "quantitative models for shape, location and dynamics of personal space are interesting opportunities for collaborative research."

1.1 The PTR Model

The Physical Trust Requirement (PTR) model is a recently proposed theory [4] which generates the sizes of circular proxemic zones from the kinematics of potential collisions between two agents, as represented in Fig. 1. PTR is defined as a Boolean property of the physical state of the world (not of the psychology of the agents) with respect to Agent_1 during an interaction, true if and only if Agent_1's future utility is affected by an immediate decision made by Agent_2.

PTR is calculated from the perspective of Agent_1 and generates the proxemic zones for Agent_1 as Agent_1 is being approached by, and trying to avoid collision with, Agent_2. The zones are not symmetric between Agent_1 and Agent_2. Agent_2 has its own zones which must be calculated separately by flipping their roles. Agent_1's zones are generated as follows:

The *Intimate zone* is the region actually occupied by Agent_1, so that Agent_2 entering it is an actual collision. Humans allow only close family into this zone to allow hugging or other forms of contact. Under the PTR model, they would in general be vulnerable to harm when contact occurs but are confident that this will not happen from close family.

The Personal zone, may be identified with the PTR model's *Crash zone*, the region close to Agent_1, $\{d : 0 < d < d_{crash}\}$,

$$d_{crash} = v_2 t_2 + \frac{v_2^2}{2a_2}, \tag{1}$$

in which a crash is guaranteed and neither party can prevent it. v_2 is Agent_2's speed. The first term depends on Agent_2 thinking reaction time, t_2, and the second term represents the physical braking distance, a_2 is the maximum available

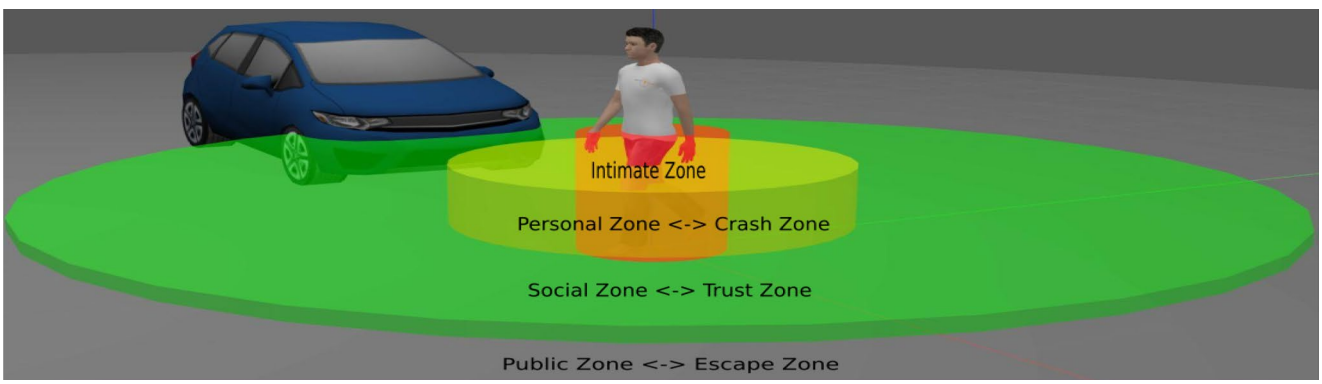

Fig. 1 Vehicle entering pedestrian's social zone, which has been identified with the trust zone generated by the PTR model [4, 6]

deceleration of Agent_2 (which for wheeled vehicles is usually assumed to be $\mu_2 g$ where μ_2 is the coefficient of friction between Agent_2's tyres and tarmac, and g is Earth's gravitational acceleration $9.81\,\text{m/s}^2$ [7]). Humans allow family members and personal friends into this zone. The PTR model would interpret this as the friends here being able to initiate mutually unavoidable contact if they choose to, with no option for Agent_1 to escape, but the friends are trusted that any such contact would be benevolent such as a brief handshake or pat. As such actions are irreversible once begun, they do not create any power relationship between the agents: if Agent_2 begins the action, they cannot bargain to retract it in return for concessions from Agent_1.

The Public zone may be identified with the *Escape zone* of the PTR model, the area where Agent_1 is able to choose their own action to avoid the collision, without needing to trust Agent_2 to behave in any particular way. If w_2 is the width of Agent_2, which Agent_1 must cross at speed v_1 if they wish to pass first, and t_1 is Agent_1's thinking reaction time needed to notice Agent_2 and initiate a response, then the escape zone is then $\{d : d_{escape} < d\}$ with

$$d_{escape} = v_2 t_1 + w_2 \frac{v_2}{v_1}. \tag{2}$$

The *Social zone* may be identified with the *Trust zone* of the PTR model, the region $\{d : d_{crash} < d < d_{escape}\}$ where the PTR is true. Agent_2 can here *choose* to slow down to prevent collision, but Agent_1 is incapable of taking any action to affect this outcome themselves. This occurs when Agent_1 cannot get out of Agent_2's way in time to avoid collision, but Agent_2 may choose to slow and yield to prevent the collision. This is the most interesting zone for HRI applications, because it is where trust is required between strangers. Humans may allow colleagues and business associates to enter, but doing so creates a requirement of trust between them. In this zone, Agent_2 can choose to initiate harm to Agent_1 and also retain the ability to retract such an action – thus wielding power over Agent_1. Two humans who are not friends, each allowing the other to enter their social zones is thus an act of mutual trust. Such an act may be performed deliberately to strengthen a desired relationship such as a business deal. However, it is otherwise undesirable to allow a stranger into this zone due to the vulnerability which arises. It is this discomfort which has been suggested as a suitable negative utility for the sequential chicken model.

The PTR model parameters can be fit to generate the proxemic zones to within 1% quantitative accuracy of their empirical observations by using realistic and typical values from two simulated pedestrian agents sizes and speeds [6]. It has also been shown how zones for variants of this model can be generated, including for human-human interactions, and human-humanoid robot interactions in cases where Agent_1 begins facing at different angles to Agent_2 and the effect of that start heading [6].

1.2 Contributions

The heading models in [6] assumed unrealistic dynamics in which Agent_1 first turns on the spot and then moves in a straight line, and suggested that future work should refine this assumption. This paper first reviews recent relevant empirical findings in the area which suggest that proxemic zones shapes are non-circular due to these heading effects. It updates the PTR model with new assumptions based on these findings. It then solves the new model, finding new analytic solutions to reproduce some of the empirical observations. This work aims to determine the proxemic zone shapes and sizes for dual moving agents, using simulation and analytic approximation. Recent work [8] proposed some first analytic models for the outer boundary (d_{esc}) only of the social zone, which are extended here with new understanding of the analytic approximation assumed, solutions for the inner boundary (d_{crash}), new and numerical simulation results. Validation of the simulation against analytic approximation then also allows simulation of new, more complex strategies which may not possess analytic solutions.

2 Empirical Evidence for Proxemics Zone Shapes

This section reviews recent relevant empirical findings in the area of proxemic zone shapes.

2.1 Circular Proxemics Zone Shapes

Hall's theory [3] defined the four proxemic zones as concentric circles, and several empirical research works have used these circular proxemic zone shapes . For example, Koay et al. [9] used the proxemic results from their previous studies that take into account the distance and approaching angle and showed that proxemic zones are of a circular shape. Aghaei et al. [10] developed a vision method to detect social distancing policy using a single image. In their work, the proxemics zones are represented as discs on the floor, thus with a circular shape.

Tatarian et al. [11] used a circular shape for proxemics zones and divided them into three distinct roles for group interactions: the *transactional zone* where objects in that area are in the person's implicit target attention, the *front zone* is in front of the person and the *gaze zone* is where people's gaze meet. Gao et al. [12] developed an end-to-end deep learning model to learn human proxemic preferences

for a robot moving towards participants from the quarter of a circle. Satake et al. [13] investigated robot approaching strategies from different distances towards humans. Their work using Hall concentric proxemic zones showed how a robot can begin an interaction with a human, i.e. communicate via its position that it wants to start interacting with them.

2.2 Non-Circular Proxemic Zone Shapes

Unlike the works cited in the previous section, several studies have shown that proxemic zones are of different shapes. Duncan and Murphy [15] reviewed 16 environmental, personal and agent factors that affect proxemic distances in human-human and human-robot interactions, and based on which they introduced a model of comfortable distance. Hans and Hans [16] reviewed three aspects of non-verbal communication that are important in human interactions, namely proxemics, kinesics and haptics.

2.2.1 Elliptical Zones

In the social force model [17] often used to describe multiple agents interaction dynamics, personal space is part of the pedestrian's private sphere thus resulting into repulsive forces towards strangers in order to reduce uncomfortable situations. The proxemic zones can thus be modelled in this case by concentric ellipses according to [5]. Lehmann et al. [18] measured human proxemic preferences with the small NAO robot with the assumption that the intimate zone is circular while the personal, social and public zones are elliptical. Jimenez et al. [19] proposed elliptic zone shapes for the interpersonal-social zone and the interpersonal-public zone used in a smart walker with social conventions. Kirks et al. [20] modelled and controlled interactions between workers and a socially interacting robot in a factory by using elliptic, worker dependent proxemic zones in free navigation.

2.2.2 Laterally Asymmetrical Zones

Gérin-Lajoie et al. [21] showed that proxemic zone shapes are laterally asymmetrical during obstacle avoidance, with some subjects tolerating a reduced personal space in their dominant side, as shown in Fig. 2(e).

2.2.3 Egg-Shaped Zones

Hayduk [22] were among the first to question the widely accepted circular zones. They investigated the 2D shape of personal space and found that egg-shaped (ovoid) zones best describe human proxemic zones, with a larger frontal space and smaller rear space, and found no difference in between genders. Kosinski et al. [23] investigated human perceived comfort level based on a robot approaching distance and angle via a set of rules, fuzzy sets and parameters. It was assumed that the approaching distance and angle can be described by sigmoid and bell-shaped functions and that the perceived comfort decreases as the angle changes. The authors found that the proxemic distance is linked to the angle of approach and that subjects feel more comfortable with approaches from the boundary of their field of view. Participants were more tolerant when the robot approached from the right hand side and felt least comfortable when the robot approached straight ahead.

Adams and Zuckerman [24] studied the proxemic space requirements of female American students under bright and dark conditions. Their results showed that the shape of the personal space zones change and the rear distances are greater than frontal distances. But previous work [25, 26] found similar distances for normal subjects whereas [27] findings were for violent prisoners. In particular, Strube and Werner [26] made a clear distinction between interpersonal distance which is the observable distance between two people and the personal space or proxemics is described as a more "cognitive and subjective" distance that is not directly

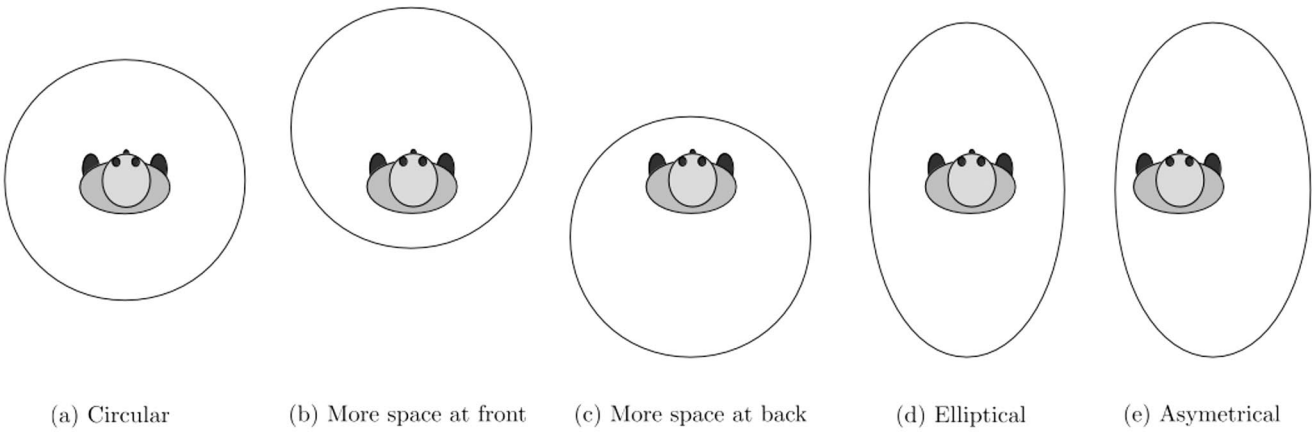

Fig. 2 Types of proxemics zones shapes, from [5, 14]

observable to both interactants. However, the authors found that both the interpersonal distance and personal space expand in response to a threat.

Daza et al. [28] used a symmetric Gaussian function to represent proxemic zones, with the intimate zone corresponding to the peak and highest values of the function. This approach was incorporated into the robot navigation strategies around humans. Ginés Clavero et al. [29] proposed adaptive proxemic shapes based on human activities, location, culture and specific situations. They adapt the asymmetric Gaussian function from Kirby et al. [30] and vary the parameters depending on activities such as cooking, running, standing and being in the bathroom. Similarly, Sousa et al. [31] used asymmetric and adaptive Gaussians for robot navigation around groups of people. Barnaud et al. [32] reproduced Efran and Cheyne's social experiment in a robotic simulator using the proxemic model proposed by Kirby et al. [30].

Patompak et al. [33] developed an inference method to learn human proxemic preferences. Their method is based on the social force model and reinforcement learning. They argued that proxemic spaces can be limited to two zones, the first being the quality interaction area where a robot could go without creating discomfort, and the private area which is the personal space. In addition, we believe that one more area is needed to model the trust relationship between humans and robots.

Mead et al. [34] also investigated the influence of proxemics on human speech and gestures and measured how that impacts on the robot speech and gesture production. Their study consisted in recruiting 10 interacting pairs of participants who didn't know each other, and each participant also interacting with a robot (PR2). Their result for human–human interactions (HHI), with mean = 1.44 m and std = 0.34 m, was consistent with previous studies but the HRI result, with mean = 0.94 m, std = 0.61 m, was much larger than in previous studies, which could be explained by the presence of robot gestures. They reported (their Fig. 10) an egg-shaped zone of preferred interaction locations, centered in front of the subject.

Torta et al. [35] performed two psychometric experiments with subjects interacting with the small humanoid robot (Nao), and proposed a parametric model of the personal space based on the results of these experiments. The model takes into account the distance and the direction of approach, and was evaluated with a user study where subjects are sitting or standing and being approached by the robot that they can stop when it reaches a comfortable distance for communication. They reported (their Fig. 9) that a human when approached by the robot from different angles has an egg-shaped comfort zone shape, centered in front of the subject.

Neggers et al. [14] showed that "experimental research on how robots can avoid a person in a comfortable way is largely missing". Their empirical findings suggest that the outer proxemics zone shape is not circular and that passing at the back of a person is more uncomfortable compared to passing at the front. Their results showed an empirical 'comfort zone', possibly equivalent to the inverse of a Hall zone, which matches the egg shapes expected.

Fig. 2 shows a summary of the different proxemic zone shapes reviewed above. It appears from surveying the related work that many studies are in favour of egg-shaped zones to best describe human proxemics.

3 Methods

Agent motions, including of pedestrians, can be modeled in different ways, and different assumptions about forward and rotational motion may give rise to different zone shapes. In general, agents may be human walkers, human drivers, or autonomous vehicles or robots with various types of steering capabilities and strategies. We will consider and model various strategies.

The environment is the same in all strategies as shown in Fig. 3: Agent_1 (for example, a pedestrian) begins at the coordinates' origin, oriented at angle θ from the approach of Agent_2 (for example, a car, robot, or another pedestrian) along the x-axis. (i.e. at $\theta = 0$ the agents are facing each other; at $\theta = \pi$ they are both oriented in the same world direction). Both agents are assumed to be circular with width (diameter) w_1 and w_2 for Agent_1 and Agent_2. It will be useful to define the average width of the two agents,

$$w = \frac{w_1 + w_2}{2}. \tag{3}$$

The two agents are just touching when their centers are distance w apart.

Agent_2 begins at $y = 0$, $-x_{start}$ traveling at speed v_2 along the x-axis towards the origin (Agent_1's starting position). Define the *collision corridor* as the area swept out by Agent_2's path if Agent_2 travels forwards infinitely.

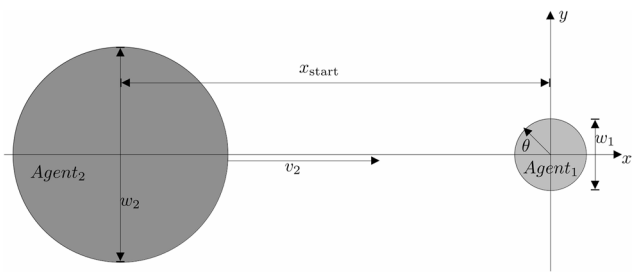

Fig. 3 Environment setup

Agent$_2$ may or may not brake, and if braking, can do so by applying deceleration a_2 after thinking time t_2. Agent$_1$ then attempts to avoid collision by escaping from the collision corridor formed by Agent$_2$'s path, using its maximum linear speed v_1 and maximum angular velocity ω_1 in different strategies. Agent$_1$ may begin to escape after thinking time t_1.

For large x_{start}, Agent$_1$ can escape, while for small x_{start}, a collision will occur. We wish to find the value of x_{start} at which this transition occurs, as it forms a proxemic zone boundary. The inner trust boundary, (crash distance, d_{crash}) is found when Agent$_2$ is braking (i.e. collision avoidance is due to Agent$_2$'s action) and the outer boundary (escape distance, d_{esc}) is found when Agent$_2$ is not braking (i.e. the collision avoidance is entirely due to Agent$_1$'s actions). Agent$_2$ is assumed to approach in a straight line directly towards Agent$_1$

We plot quantitative proxemic zones for a human Agent$_1$ being approached by another human Agent$_2$, using the PTR model. Unlike previous work, we will now take account of the initial heading of Agent$_1$ relative to the direction of approach by Agent$_2$, and of various possible strategies that Agent$_1$ could use to optimise their escape in order to reduce the zone sizes. We will also sometimes be able to obtain and plot analytically exact or approximate solutions.

For interactions between two humans, we assume parameters based on standard values used in the literature: circular diameter $w_1 = w_2 = 0.9\text{m}$ (to fit the empirical intimate zone); maximum walking speed $v_1 = v_2 = 1.4\text{m/s}$, maximum turning speed $\omega_1 = 1.0\text{rad/s}$, maximum deceleration $a_2 = 5\text{m/s}^2 \approx 0.5g$, and thinking times $t_1 = t_2 = 1.0$ s.

We use the notational convention that variables that change over time are written explicitly as functions of time, such as the speed of Agent$_1$ at time t by $v_1(t)$, while allowing constants with the same name but no argument to co-exist with the functions, such as v_1 meaning a particular speed of interest.

3.1 Simulations

We here use numerical simulation to approximate the social zone shape, using the same parameters as the analytic setup. Simulations are useful for two purposes: first, as a validation that the analytic results are correct; and second, to obtain approximate results for more complex strategies in which analytic solutions are not easily obtainable.

The basic simulation setup is illustrated in Fig. 4. The white dots mark 1 m squares to show scale. The center of the grid is the origin. x runs rightward from the origin and y runs up. Angles are measured anticlockwise from the x axis.

The simulation is implemented in *pygame*, a 2D game library. For a given scenario, two agents are moved to represent the subject and other. The scenario ends either if Agent$_1$ escapes from the path of Agent$_2$, or if their circles collide (these are visualized as sprites but modeled for collision detection as circles, matching the analytic models). Define an *experiment* as fixing the values and functions of all simulation components except for θ and x_{start} and the boolean controlling whether Agent$_2$ breaks or not. To run an experiment, many discrete values of θ are tried, and for each one, a binary search is performed over x_{start} to find the transition between collide and escape outcomes. This search is performed twice, once with Agent$_2$ braking and once not braking. An experiment thus takes several minutes of real-time computation, and results in finding the social zone boundaries as a function of initial Agent$_1$ heading.

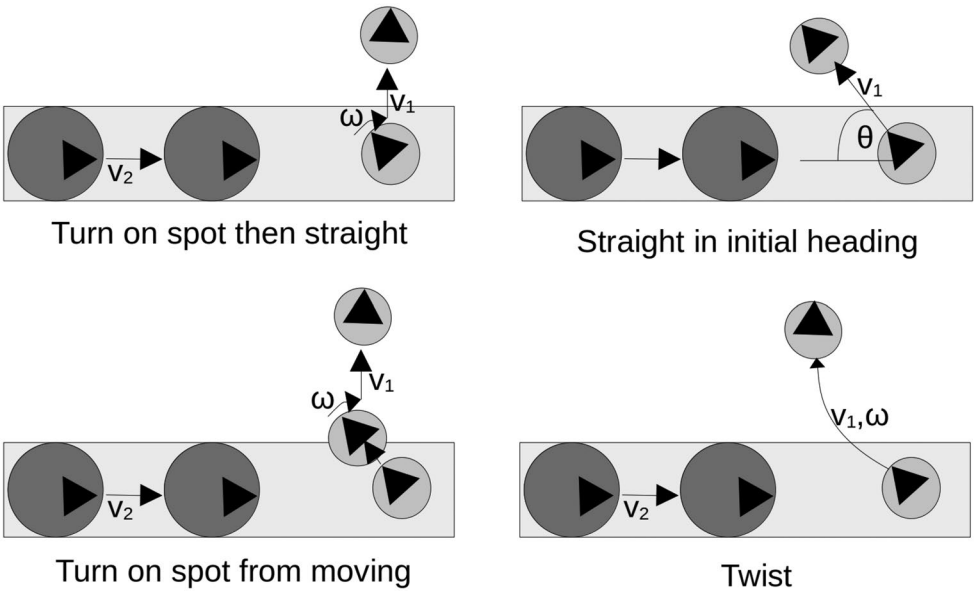

Fig. 4 Geometries of the different strategies tested. In each strategy, Agent$_2$ is the darker circle, moving horizontally from left to right. Agent$_1$ is the lighter circle. The rectangle is the collision corridor

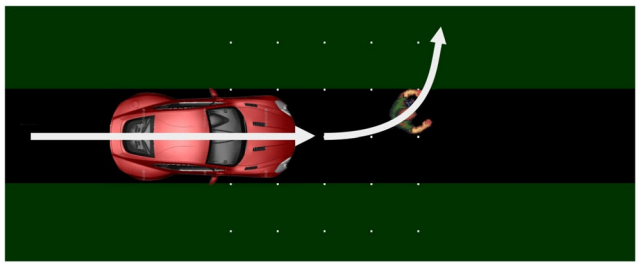

Fig. 5 Simulation screenshot

3.2 Analytic Derivations

Exact analytic solutions may be obtainable in some cases. We will show how to set up and solve these where possible. In other cases, approximations are used to obtain analytic solutions. Analytic and simulation results are checked against each other to find and remove software and algebra errors and to check the realism of analytic approximations.

4 Motion Strategies

We consider various strategies that Agent_1 may use in the interaction, as illustrated in Fig. 5. Strategy used by Agent_1 may depend on mechanical constraints – such as whether the agent has legs or wheels – as well as their choice.

4.1 Strategy: Instant Turn on Spot

This first, baseline, strategy assumes that Agent_1 may turn on the spot to any heading instantaneously, then move forwards in a straight line. Regardless of initial heading, the optimal strategy is [6] thus always to rotate to face orthogonally to Agent_2, then walk straight forwards to escape.][1]

4.1.1 Escape Distance

The escape distance d_{esc} is the shortest starting distance between the two agents' centers which results in them colliding, i.e. reaching a configuration in which their centers are distance w apart, when Agent_2 *does not* act (brake) to avoid collision.

The time taken for Agent_1 to completely exit from the collision corridor, $\tilde{\tau}$, is Agent_1's thinking time plus the time spent traveling distance w at speed v_1,

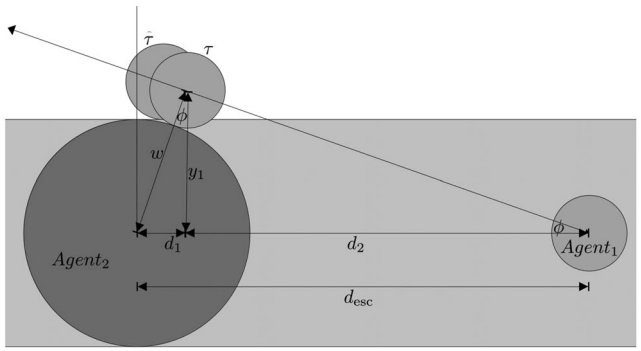

Fig. 6 Geometry of infinitesimal collision for escape, in Agent_2 frame

$$\tilde{\tau} = t_1 + \frac{w}{v_1} \tag{4}$$

However, as we have assumed that both agents are circular, this is not the first time at which the two agents can touch. Touching instead occurs slightly earlier, at some time τ, before the center of Agent_2 has reached Agent_1's starting location, as shown in Agent_2's frame of reference in Fig. 6. The angle θ depends on how far the two agents have traveled to reach the collision.

Choose our clock so that time $t = 0$ occurs at the moment that Agent_1 finishes thinking, and τ is time elapsed between $t = 0$ and collision.

In Agent_2's frame of reference, Agent_2 appears stationary, and Agent_1 appears to have horizontal speed of v_2 during the whole interaction, as well as vertical speed v_1. At time τ of collision, Agent_1 will have moved horizontal distance d_2 as

$$d_2 = v_2\tau. \tag{5}$$

As we started the clock after Agent_1's thinking, Agent_1 will also move vertically by

$$y_1 = v_1\tau, \tag{6}$$

We have

$$\tan\phi = \frac{y_1}{d_2}. \tag{7}$$

From Eqs. 5 and 6, we thus get

$$\tan\phi = \frac{v_1}{v_2} \tag{8}$$

so

$$\phi = \tan^{-1}\left(\frac{v_1}{v_2}\right). \tag{9}$$

[1] This is an improved version of the model studied in [6] option 1, replacing its wheel friction model with a general deceleration term, adding some further mathematical detail to include the widths of the agents, and thinking times and to cover cases in which Agent_2 may stop before reaching Agent_1, and presenting the results visually in a new polar form so they can be viewed directly as proxemic zones.

The first contact occurs when their centers are distance w apart. w forms the hypotenuse of two right-angled triangles, and by basic geometry θ can be found in each of them, so that

$$d_1 = w\sin(\phi) = w\frac{v_1}{\sqrt{v_1^2+v_2^2}}, \tag{10}$$

$$y_1 = w\cos(\phi) = w\frac{v_2}{\sqrt{v_1^2+v_2^2}}. \tag{11}$$

From this we can find the value of the collision time,

$$\tau = \frac{y_1}{v_1} = \frac{w}{v_1}\frac{v_2}{\sqrt{v_1^2+v_2^2}}. \tag{12}$$

Agent_2 also moved a further $v_2 t_1$ before we started our clock, while Agent_1 was thinking. Agent_2 has thus moved in total

$$d_2 = v_2 t_1 + v_2\tau = v_2 t_1 + \frac{w}{v_1}\frac{v_2^2}{\sqrt{v_1^2+v_2^2}}. \tag{13}$$

This is not quite the escape distance because we need to add a distance of d_1 as a buffer between the two agents. The escape distance is thus

$$d_{esc} = d_2 + d_1 = v_2 t_1 + \frac{w}{\sqrt{v_1^2+v_2^2}}(\frac{v_2^2}{v_1} + v_1). \tag{14}$$

4.1.2 Crash Distance

The crash distance d_{crash} is the shortest starting distance between the two agents' centers which results in them colliding, i.e. reaching a configuration in which their centers are distance w apart, when Agent_2 *does* act (brake) to avoid collision.

Here we will choose a different clock which fixes $t = 0$ at the start of the scenario, when both agents start thinking. We will work in the world frame (rather than Agent_2's frame used previously) as shown in Fig. 7.

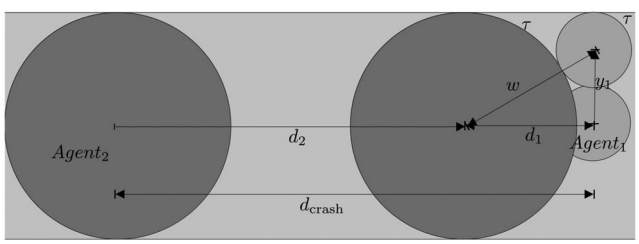

Fig. 7 Geometry of infinitesimal collision for crash, in world frame

Let H be the Heaviside step function. Its integral is then $xH(x)$, the ramp/rectifier/relu function. Its double integral is, $\frac{1}{2}x^2H(x)$, the positive-half quadratic function.

Agent_1 motion is given by:

$$v_1(t) = v_1 H(t - t_1), \tag{15}$$

$$y_1(t) = \int_0^t v_1(t)dt = v_1(t - t_1)H(t - t_1). \tag{16}$$

Agent_2 motion is defined by its starting speed and acceleration profile:

$$v_2(t = 0) = v_2, \tag{17}$$

$$a_2(t) = (H(t - t_2) - H(t - (t_2 + v_2/a_2)))a_2. \tag{18}$$

This is because the rightmost H is only nonzero after Agent_2's stopping time, $(t_2 + v_2/a_2)$, and there counters out the previous H term, to model Agent_2 remaining stationary once its braking is complete (rather than continuing to accelerate and move backwards). This stopping time is an upper bound on the collision time. So we can restrict our consideration of t to the interval $t \in [0, (t_2 + v_2/a_2)]$. This enables us to drop that term so that for the restricted times considered,

$$a_2(t) = a_2 H(t - t_2) \tag{19}$$

$$v_2(t) = v_2 - \int_0^t a_2(t)dt \tag{20}$$

$$= v_2 - a_2(t - t_2)H(t - t_2) \tag{21}$$

$$d_2(t) = \int_0^t v_2(t)dt \tag{22}$$

$$= v_2 t - \frac{a_2}{2}(t - t_2)^2 H(t - t_2). \tag{23}$$

Define collision time $t = \tau$ to be the first time at which the two agents are touching under these dynamics, as in Fig. 7, i.e. by Pythagoras,

$$d_1^2(\tau) = w^2 - y_1^2(\tau) = (d_{crash} - d_2(\tau))^2 \tag{24}$$

This cannot be solved analytically for (τ, d_{crash}) because it is quartic. It is thus useful to move to either analytic approximation or to numerical simulation at this point, and we next consider both of these approaches.

4.1.3 Corridor-Exit Approximation

While the above gives the exact analytic crash zone, it is not especially useful in aiding human understanding of its properties because it relies on a numerical solution step. To gain further insight into the model, it is useful to consider an approximation which has a simpler and more understandable form.

One such approximation can be made by assuming that the moment of minimal collision occurs at $\tilde{\tau}$ rather than at τ, as shown in Fig. 8. By assuming (falsely) that no collision can take place before corridor exit, the geometry becomes much simpler, because collision now occurs when Agent_2 has reached exactly Agent_1's starting point, removing the need to calculate $d_1 \approx 0$ and $\phi \approx 0$. This assumption will be especially useful in later more complex strategies but is first tested here.

The largest possible error in this approximation is w, because this is the largest possible horizontal difference between agent positions that can remain consistent with their centers being w apart as required for collision. The approximation is most accurate when $v_2 \gg v_1$ because this is where ϕ actually tends towards 0. For example, this would be the case if Agent_1 is a slow pedestrian and Agent_2 is a fast car.

To calculate d_{crash} using this approximation: on Agent_1 corridor exist, Agent_2 has traveled $d_2(\tilde{\tau})$ to reach the collision point, which under

$$\begin{aligned} d_{crash} &\approx d_2(\tilde{\tau}) \\ &= v_2\tilde{\tau} - \frac{a_2}{2}(\tilde{\tau} - t_2)^2 H(\tilde{\tau} - t_2) \\ &+ \frac{a_2}{2}(\tilde{\tau} - (t_2 + v_2/a_2))^2 H(\tilde{\tau} - (t_2 + v_2/a_2)) \end{aligned} \tag{25}$$

We know that Agent_2's stopping distance is an upper bound on d_{crash}. So we can drop the rightmost term, which only has any effect at times after Agent_2's stopping time,

$$d_{crash} \approx v_2\tilde{\tau} - \frac{a_2}{2}(\tilde{\tau} - t_2)^2 H(\tilde{\tau} - t_2). \tag{26}$$

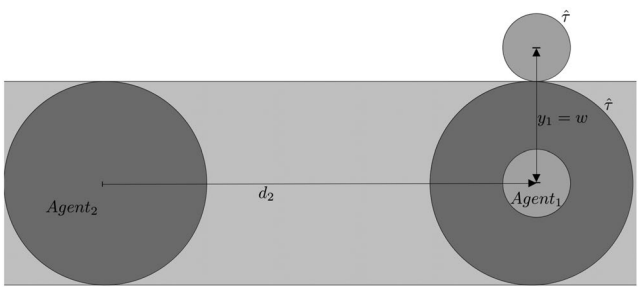

Fig. 8 Geometry of corridor exit approximation, in world frame

The H term here acts as a discrete switch. This is because there are two distinct cases in the solution. The term checks if Agent_2 has braked at all before reaching Agent_1's starting location and if so, reduces the distance by this braking. If Agent_2's thinking time is large then it is possible for Agent_2 to reach Agent_1 before Agent_2 has finished thinking or performed any braking.

4.1.4 Corridor Exit and Symmetric Agents

If, in addition to the corridor exit approximation, we also assume symmetric reaction times $t_1 = t_2 = t$ and symmetric speeds $v_1 = v_2 = v$, then we obtain simply

$$\tilde{\tau} = t + w/v \tag{27}$$

$$d_{crash} \approx v_2\tilde{\tau} - \frac{a_2}{2}(\tilde{\tau} - t_2)^2 H(\tilde{\tau} - t_2) \tag{28}$$

$$d_{crash} \approx v(t + w/v) - \frac{a_2}{2}(w/v)^2 H(\tilde{\tau} - t_2) \tag{29}$$

$$d_{crash} \approx vt + (1 - \frac{wa_2}{2v^2})w \tag{30}$$

4.1.5 Corridor Exit and Symmetric Agents and Immediate Reactions

If we further assume instant reaction times, $t = 0$ then,

$$\tilde{\tau} = w/v \tag{31}$$

$$d_{crash} \approx (1 - \frac{wa_2}{2v^2})w \tag{32}$$

If $a_2 = 0$, then $d_2 = w$. This is because Agent_2 can travel the same distance in the same time as it takes Agent_1 to leave the corridor. If a_2 is larger then d_{crash} decreases.

4.1.6 Results

The simulation and analytic results are shown in Fig. 9. The analytic escape distance is exact and agrees with simulation, while the analytic crash distance uses the corridor escape approximation so underestimates the simulation due to its assumption of changing the collision location. It is important to note here that the escape distances match between exact analytic and simulation, as this gives confidence that the simulation software is correctly implemented so that we can rely on it for more complex cases where exact analytic solutions are unavailable. Note that the pairs of subfigures do not represent Agent_1 and Agent_2. Fig. 9 and all subsequent graphs are drawn from the perspective of Agent_1,

who is being approached by Agent_2. Subfigures (a) and (b) each show both the inner and outer boundary of the social zone, with the different subfigures showing them both as computed by numerical simulation or by analytic solution.

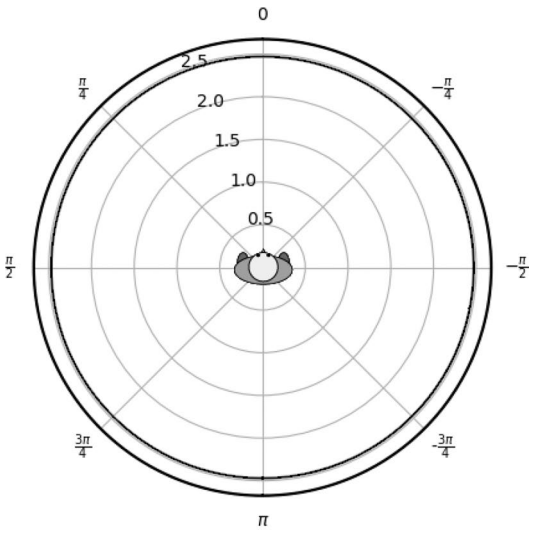

(a) Numerical simulation.

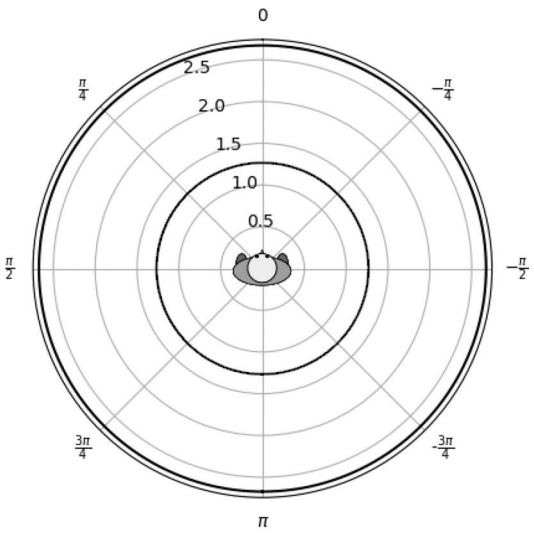

(b) Analytical solution.

Fig. 9 Strategy: instant turn on spot social zone inner and outer boundaries. In each image, the inner and outer boundaries of Agent1's social zone are shown by the thick black lines. Distances are in meters, angles in radians, centered on a pedestrian facing upwards on the page. (**a**) shows the numerical simulation results for both boundaries; (**b**) shows the analytic solution for both boundaries

4.1.7 Analysis

The escape distance has an exact analytic solution, but it is interesting to consider the escape distance as well as the crash distance under the above approximations, because they simplify the form and enable clearer comparison between the crash and escape distances.

Under the corridor exit and symmetric agents assumptions, $t_1 = t_2 = t, v_1 = v_2 = v$,

$$d_{esc} = v_2 t_1 + (w/v_1)v_2 = vt + w \tag{33}$$

This shows (under the approximations) that w is a fixed lower bound on the escape distance, which then grows linearly in v and/or t. In the limiting case of $v = 0$, the escape distance is w because the agents only collide when starting touching.

If we set $t = 0$ then d_{esc} reduces to w, independent of the speeds. This is because however long it takes Agent_1 to escape, traveling w vertically, at v will be the same time needed for Agent_2 to move w horizontally at v.

The crash distance, under the assumptions, has upper bound equal to the escape distance because $wa_2/2v^2$ is positive.

If t is large, vt dominates both the escape and crash distances, making the effect of braking small. As t nears 0, braking has a larger effect on the relative sizes of the distances.

4.2 Strategy: Turn on Spot Then Straight

This strategy was previously suggested in [8] but is presented here with the new analytic approximation understanding and verified with simulation.

In this option, Agent_1 again begins standing stationary at angle θ to Agent_2's heading. Agent_1 first turns on the spot at angular velocity ω, until they are orthogonal to Agent_2's approach, and then moves forward at speed v_1. The rotation direction is chosen to be the shortest to reach the orthogonal direction. Unlike the instant turn-on-spot strategy, the rotation now takes time, assuming angular velocity ω.

Using the same collision escape approximation as previously, the time taken for Agent_1 to escape the collision corridor is now the sum of their thinking time, turning time, and linear motion time:

$$\tilde{\tau} = t_1 + \frac{|\pi/2 - |\theta||}{\omega} + \frac{(w_1 + w_2)}{2v_1} \tag{34}$$

If Agent_2 yields or not not yield, they will travel the same $d_2(\tilde{\tau})$ as derived in the Instant Turn on the Spot strategy during this time. This is again equal to the escape distance, $d_{esc} \approx d_2$.

This strategy assumes that it is always best to take time to rotate to 90 degrees first. This seems sensible for normal humans. But for other types of agent, where the rotate speed is very slow relative to forward speed, it might be more optimal to rotate only to some smaller angle. We are thus assuming that turning is 'fast' compared to moving forwards.

Results: The resulting social zone is shown in Fig. 10. It has the same radii as instant turn on the spot if and only if $\theta = \pi/2$, with other heading having longer distances due to the extra time taken for Agent_1 to turn before moving off. The radii to the front of Agent_1 are now 1.6 m and 3.6 m. The inner boundary is still larger than the empirical 1.22 m, but the outer one is now suggestively close to the empirical 3.7 m.

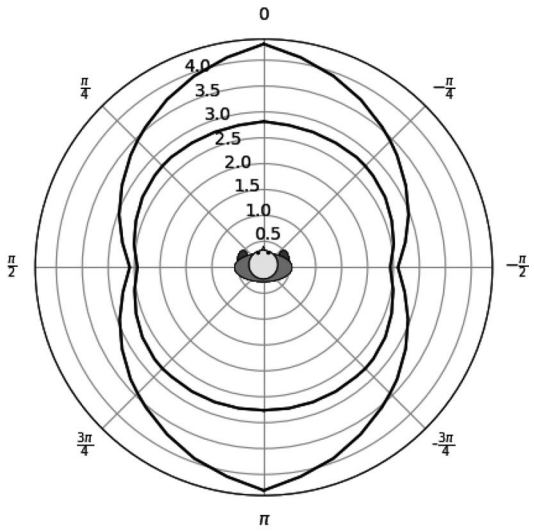

(a) Numerical simulation.

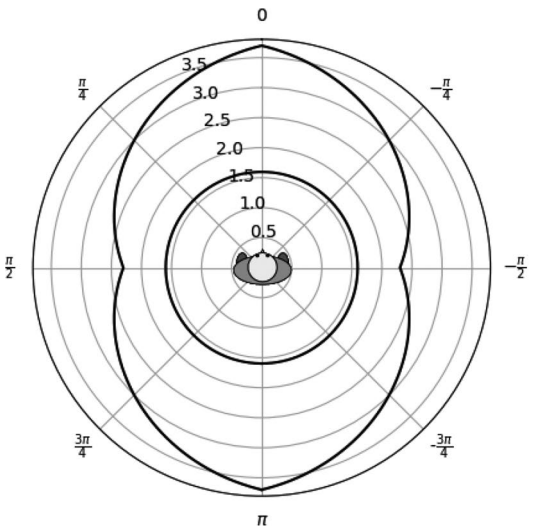

(b) Analytical solution.

Fig. 10 TurnOnSpotThenStraight social zone inner and outer boundries

Analysis: As in Instant Turn On Spot, it is not possible to make large separation of the inner and outer social boundaries if the agents' speeds and thinking times are the same and thinking times are large. Adding turning time has the same effect as a longer thinking time for Agent_1 and is able to separate out the boundaries more, with larger separations occurring towards the front. Adjusting ω controls the size of this effect.

4.3 Strategy: Straight in Initial Heading

In this strategy, Agent_1 tries to escape by moving forward in a straight line in the direction of their initial heading θ at speed v_1. They do not rotate at all. This strategy was previously suggested in [8] but is presented here with the new analytic approximation understanding and verified with simulation.

The time taken for Agent_1 to leave the collision corridor is

$$\tilde{\tau} = t_1 + \frac{(w_1 + w_2)}{v_1 |\sin(\theta)|} \tag{35}$$

If Agent_2 will travel the same $d_2(\tilde{\tau})$ as derived in the Instant Turn on the Spot strategy for the two cases (escape and crash distance) during this time.

Using the collision corridor approximation, when Agent_1 leaves the collision corridor, they have traveled an additional distance towards Agent_2,

$$d_1 = (\tilde{\tau} - t_1) v_1 \cos\theta \tag{36}$$

(For $\theta > \pi/2$, this becomes negative as Agent_1 is moving away from rather than towards Agent_2.)

So that

$$d_{esc} = d_2 + d_1. \tag{37}$$

Fig. 11 shows the resulting social zone. At $\theta = \pi/2$ the sizes are equal to Instant Turn On The Spot. The sizes go to infinity as $\theta \to 0$ or $\theta \to \pi$ because it is impossible for Agent_2 to escape if they are constrained to only move along the collision corridor's rather than out of it. None of the distances appear especially close to the standard Hall sizes.

Results: The simulation and analytic results are shown in Fig. 11.

4.4 Strategy: Turn on Spot from Moving

In this model, Agent$_1$ begins moving in their heading direction θ, and continues to do so during their thinking time, as in Straight In Initial Heading. They stop instantly, then behave as in Turn on the Spot then Straight.

During their thinking time, Agent$_1$ travels $v_1 t_1 \sin(\theta)$ vertically and $d_1 = v_1 t_1 \cos(\theta)$ horizontally (which may be positive or negative).

This vertical distance traveled reduces the remaining vertical distance needed to escape the collision corridor to $w - v_1 t_1 \sin(\theta)$.

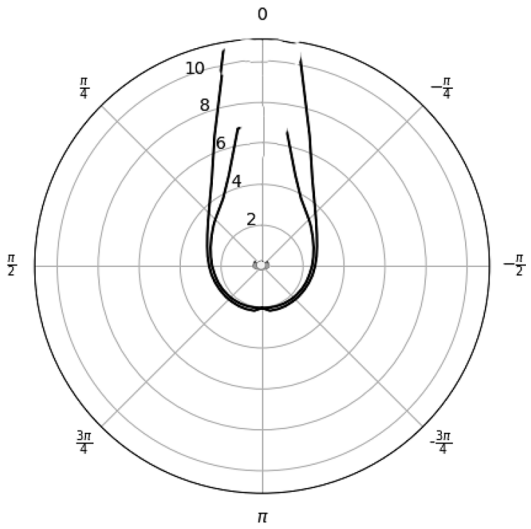

(a) Numerical simulation.

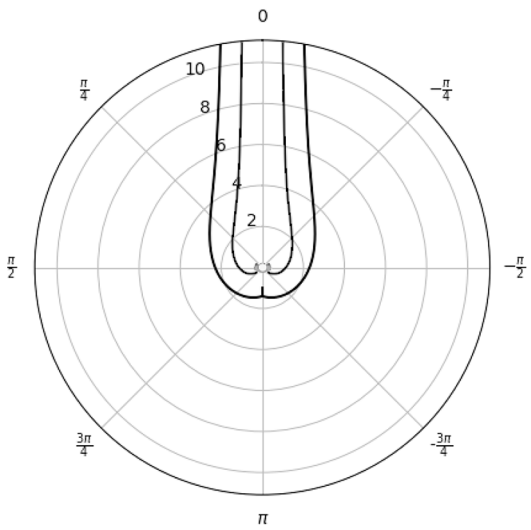

(b) Analytical solution.

Fig. 11 Straight in initial heading social zone, inner and outer boundaries

The turning time is the same as in the Turn Then Straight strategy, $|\pi/2 - |\theta||/\omega$.

The total corridor exit time is thus

$$\tilde{\tau} = t_1 + \frac{|\pi/2 - |\theta||}{\omega} + \frac{w}{v_1} - t_1 \sin(\theta) \tag{38}$$

If Agent$_2$ yields or not yield, they will travel the same $d_2(\tau)$ as derived in the Instant Turn on the Spot strategy during this time. As in Straight in Initial Heading, again with the corridor exit approximation, the escape distance is given by $d_{esc} = d_2 + d_1$.

Results: The resulting social zone is shown in Fig. 12. This is now heavily stretched out in the direction of Agent$_1$'s own motion.

4.5 Strategy: Twist

This strategy assumes that Agent$_1$ can and does turn during forward travel, where turning takes place at angular velocity ω at the same time as moving with forward velocity v_1. Twists produce arc segments of motion, around a 'great circle' whose radius is given by $R = v/\omega$. Both v_1 and ω are properties of Agent$_1$, describing how fast they can move forwards and turn. The strategy assumes that the direction (clockwise or anticlockwise) of the twist is chosen as the one which is closest to orthogonal to Agent$_2$'s approach. This strategy was previously suggested in [8] but is presented here with the new analytic approximation understanding, and verification in simulation.

Fig. 13 shows the assumed geometry of the twist strategy, annotated with the angles and lengths which will be used in the derivation. We again use the corridor exit approximation.

Agent$_1$ is trying to escape from Agent$_2$ by moving in a Twist, around the great circle of radius $r = v/\omega$. Agent$_2$ is approaching from left to right at speed v_2.

The great circle radius is determined by the properties of Agent 1,

$$R = v_1/\omega_1. \tag{39}$$

From geometry of the figure,

$$b = c - w_1/2 - w_2/2 \tag{40}$$

$$b = R\cos(\theta + \phi) \tag{41}$$

$$c = R\cos\theta \tag{42}$$

Equating the two expressions for b,

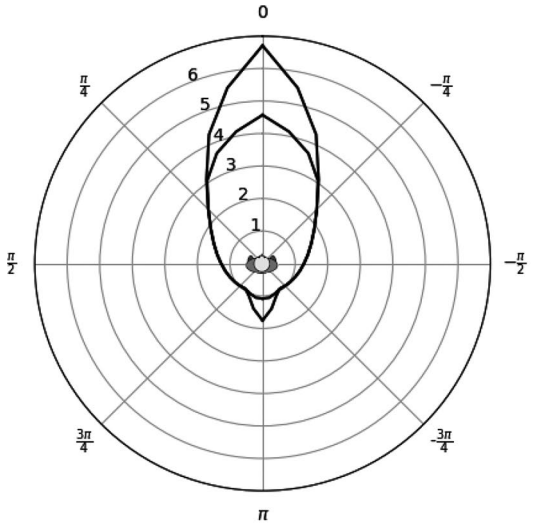

(a) Numerical simulation.

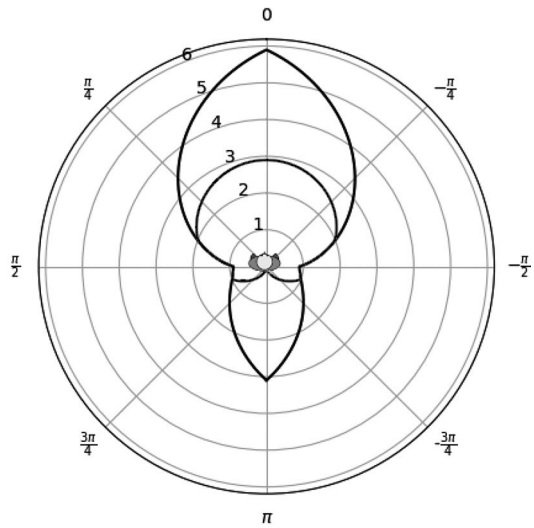

(b) Analytical solution.

Fig. 12 Turn on spot from moving, social zone inner and outer boundaries

$$R\cos(\theta+\phi) = R\cos\theta - \frac{(w_1+w_2)}{2} \tag{43}$$

$$\cos(\theta+\phi) = \cos\theta - \frac{(w_1+w_2)}{2R} \tag{44}$$

$$\phi = \cos^{-1}(\cos\theta - \frac{(w_1+w_2)}{2R}) - \theta \tag{45}$$

To think (while staying stationary), then travel ϕ around the great circle, Agent_1 takes time

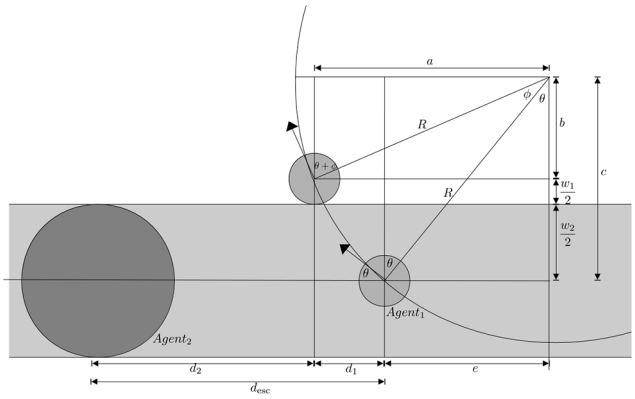

Fig. 13 Twist strategy geometry

$$\tau = t_1 + \frac{\phi}{\omega_1} \tag{46}$$

In a more detailed model, while thinking, Agent_1 could be traveling straight, as in Straight in Initial Heading.

From geometry of the figure,

$$a = R\sin(\theta+\phi) \tag{47}$$

$$e = R\sin\theta \tag{48}$$

$$d_1 = a - e \tag{49}$$

If Agent_2 yields or not not yield, they will travel the same $d_2(\tau)$ as derived in the Instant Turn on the Spot strategy during this time. As in Straight in Initial Heading, the escape distance is given by $d_{esc} = d_2 + d_1$.

If we were to consider the case having the same geometry as Fig. 13 except that Agent_2 approaches from the right rather than the left, as illustrated in Fig. 14($\pi/2$ case), then we would instead obtain:

$$d_{esc} = d_2 - d_1 \tag{50}$$

This latter case can be used, reflected, to handle cases $\pi/4 < \theta < \pi/2$.

To further improve the model, we could consider cases where Agent_1 reaches orthogonality with Agent_2 before leaving the collision corridor – as in the simulation model.

ϕ has no solution for some failure cases, as $\cos^{-1}$ is only defined on inputs in range [−1,1]. These correspond to geometries where the turning circle is too small to escape: if Agent_1 continued the twist forever, they would just walk round and round in a small circle always still in the path of the approaching Agent_2. This is illustrated in Fig. 14($w_2 < r$ failure case).

ϕ has a solution if:

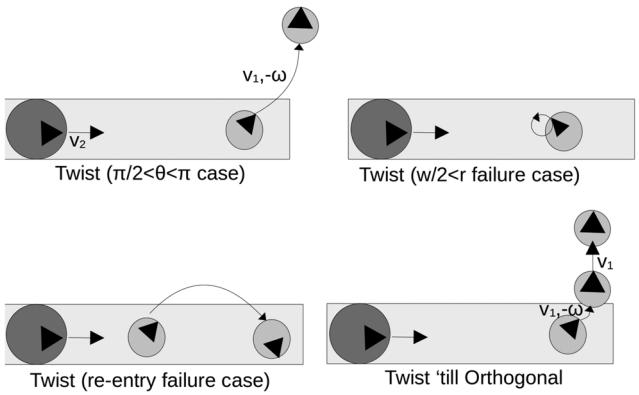

Fig. 14 Twist cases

$$-1 \leqslant \cos\theta - \frac{w_1}{r} \leqslant 1 \tag{51}$$

That gives:

$$\arccos(\frac{w_1}{r} + 1) \leqslant \theta \leqslant \arccos(\frac{w_1}{r} - 1) \tag{52}$$

Then, we have:

$$\frac{w_1}{r} - 1 \geqslant -1 \quad \text{and} \quad \frac{w_1}{r} - 1 \leqslant 1 \tag{53}$$

$$\frac{w_1}{r} \geqslant 0 \quad \text{and} \quad \frac{w_1}{r} \leqslant 2 \tag{54}$$

$$\frac{w_1}{r} \geqslant 0 \quad \text{and} \quad r \geqslant \frac{w_1}{2} \tag{55}$$

Results: Simulation and analytic results for the twist strategy are shown in Fig. 15. There is a discontinuity at $\pi/2$ because this is where Agent_1 switches from twisting clockwise to anticlockwise, changing the sign of d_2.

4.6 Strategy: Twist Till Orthogonal

Despite its excellent fit in the forward direction, the above Twist strategy has two problems. First, the lack of solutions for small R due to twists not leaving the corridor as in Fig. 14 ($w_2 < r$ failure case). Second, some twists can leave the corridor but then re-enter it as the great circle overlaps the corridor in two places, as in Fig. 14 re-entry failure). The derived solution ignores this possibility but in reality it could result in a collision in a second location. These problems become particularly acute for θ close to π and result in the discontinuities and divergence to infinities in Fig. 15.

To remove these problems, we consider a new, more advanced twisting strategy, shown in Fig. 14(Twist till Orthogonal). Here, Agent_1 begins by twisting as above, but when they reach a heading of $\pi/2$ they switch to moving in a straight line, which is the fastest way to exit the corridor.

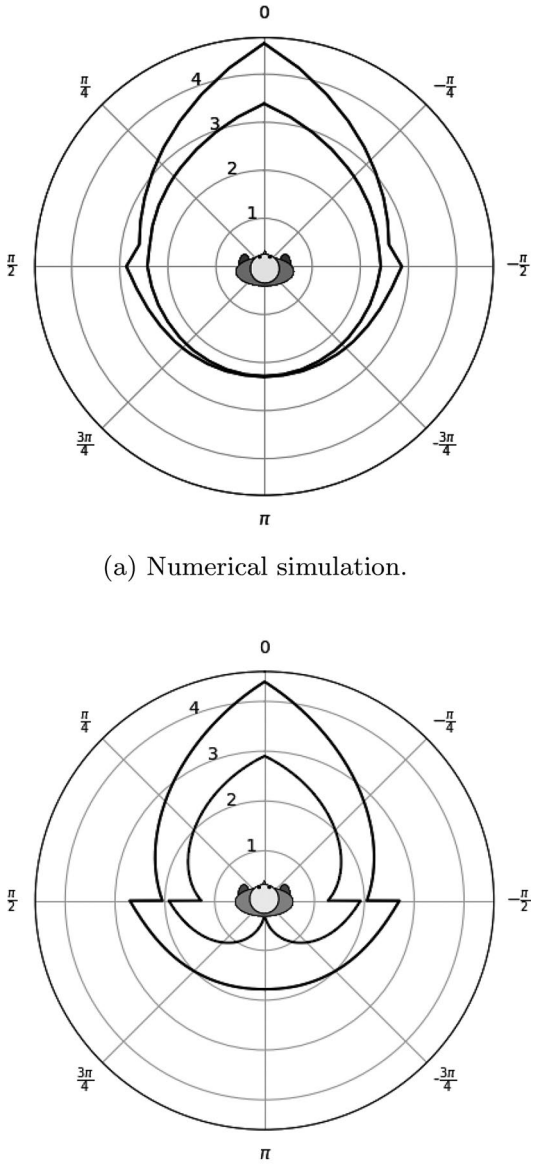

(a) Numerical simulation.

(b) Analytical solution.

Fig. 15 Twist strategy social zone inner and outer boundaries

Obtaining an analytic solution for this strategy would be more complicated than the others presented, so we here switch to numerical simulation.

Results: The result of the simulation is shown in Fig. 16 and can be seen to be similar to the simple Twist result but with artifacts resulting from those issues removed to produce a simpler shape. It approximately fits the classical circular zone radii and also matches the egg shapes assumed by Kirby [30].

This strategy may be the optimal one as it has a similar structure to Dubins paths [36], known to be optimal for agents with speed and steering to move from one pose to another. Straight In Initial Heading is the limit of Twist till Orthogonal as $R \to \infty$; while Turn-on-the-Spot then Straight is the limiting case as $R \to 0$ – the same setting in which the simple Twist strategy fails.

4.6.1 HRI Examples

As Twist until Orthogonal then Straight may be the best strategy, it is of interest to calculate and view results for variant scenarios using it. For example, Fig. 17 shows the social zone boundaries when Agent_1 is a pedestrian with the same parameters as before, but Agent_2 is replaced by a car starting from speeds $v_2 = 10$mph or 30mph, with width $w_2 = 2$m and braking $a_2 = 2\text{m/s}^2$. It can be seen that the zone increases greatly in size, and is comparable to the recommended stopping distance for the driver (e.g. in the UK: 23 m at 30mph). This suggests that the safe vehicle spacings taught to drivers (such as via the 'two second rule') can be viewed as proxemic zones for human drivers, replacing their usual human body's zones.

It is also of interest to consider zones when both agents are physically human-like robots with the same parameters as humans, except for having additional sensors and computation ability that reduce their thinking time to near-zero. Fig. 18 shows how the zones of Fig. 16 contract in this case. This raises the question of whether such robots should be programmed to deliberately delay their thinking time to create more familiar, human-like zones and interactions.

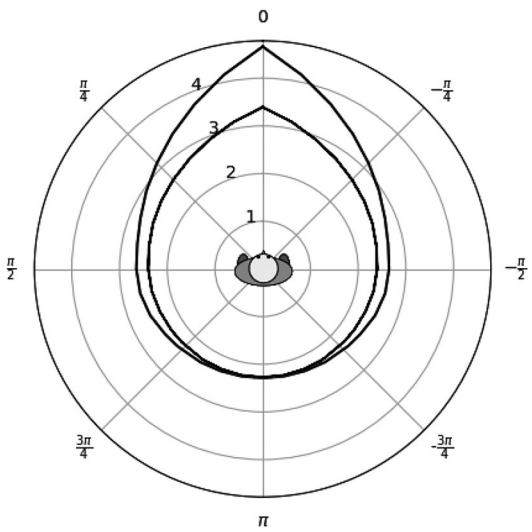

Fig. 16 Twist till orthogonal, social zone inner and outer boundaries, numerical simulation

4.7 Strategy: Sidestep-Backstep

This strategy allows the subject to move backwards, sideways, or in any other direction, without having to change heading. We assume that the walking speed decreases linearly with the direction ϕ away from the heading direction θ, as $v = 1.1 - |\theta - \phi|/\pi$. This may be a more appropriate model for human pedestrians, who for example often step backwards when aborting a road crossing attempt.

Simulation results are shown in Fig. 19.

5 Discussion

The kinematic models provide explanations for the non-circular proxemic zone deformations previously observed empirically [22, 35] and assumed by robotics models such as Kirby [30]. Our approach also uses three of the four factors that have been identified by [15] for an agent's proxemics behaviour: the angle of approach, height or size of the agent and the speed. The fourth factor is eye gaze, which we cannot model here but that could form part of future empirical experiments.

The standard circular zones that have been empirically described by Hall [3] and used in many subsequent works appear to match our Instant Turn On Spot kinematics. Elliptical zones have also been observed empirically and used in [18–20, 31] and it may be a best fit to our Turn On Spot Then Straight kinematics. Egg-shaped zones have further been observed empirically in [14, 22–24, 34, 35] and assumed in ad-hoc models [28, 30]. This pattern is best fit by our Turn on Spot From Moving and Twist Till Orthogonal kinematics.

It is possible that these two different shapes – elliptical and egg-shaped – may arise due to differences in the experimental protocols used. If the agents are restricted or encouraged to move under different kinematics then the new models would explain why these generate different zone shapes. This includes both the movements of human subjects and of the other agents – human, vehicle, or humanoid – with which they interact and mentally model and predict. We might expect human subjects to assume that wheeled robots will move as Twists, and to behave accordingly; while assuming that other humans and humanoids can also sidestep and backstep.

For example, on one hand the proxemics zones are elliptical in [18–20, 31] where they mainly consider social dynamics from the social force model perspective, with agents either attracting or repelling each other. On the other hand, the egg-shaped findings in [35] showed that the angle of approach, the size of the robot and the side from which it approaches people have an effect on the proxemics zone

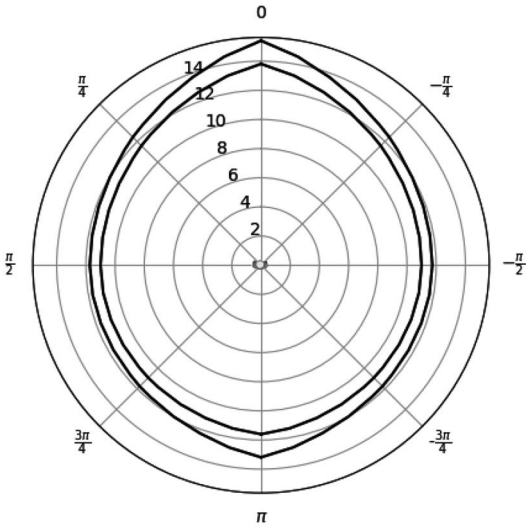

(a) 10mph Numerical simulation.

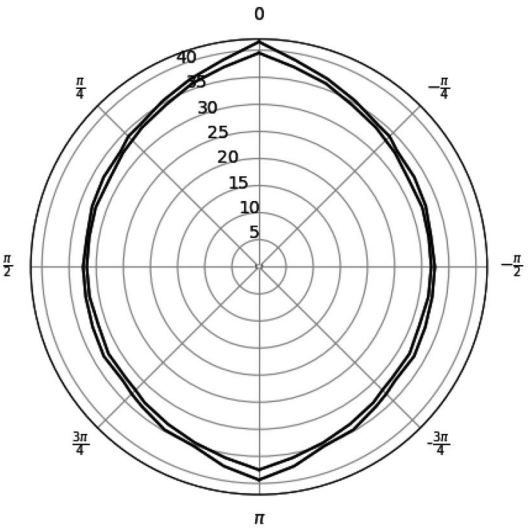

(b) 30 mph Numerical simulation

Fig. 17 Twist till orthogonal then straight, Agent_1's social zone inner and outer boundaries, simulation result, with Agent_2 replaced by a car starting at speed 10mph (**a**) or 30mph(**b**)

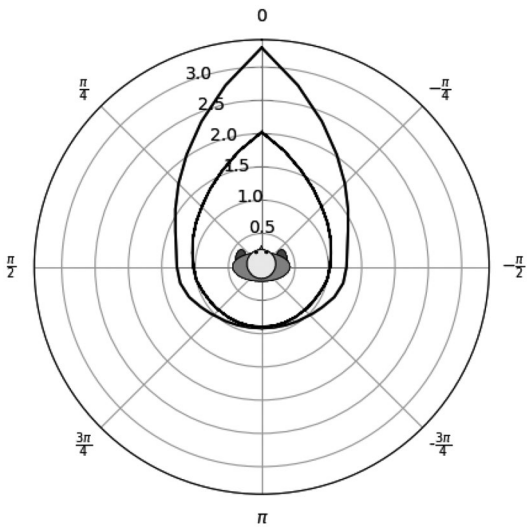

Fig. 18 Twist till Orthogonal with zero thinking times, numerical simulation

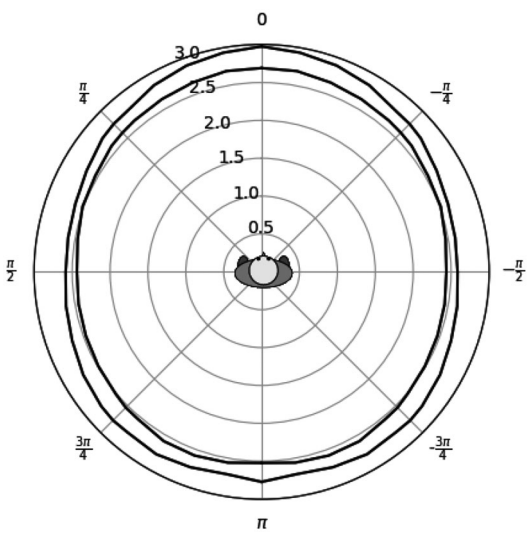

Fig. 19 Side and backsteps, no rotation, numerical simulation

sizes. Similarly in [22], it was empirically shown that the angle of approach and head turn change the proxemics zone size and shape dynamically, with a particular reduction in zone sizes at the rear where visibility is reduced. These appear to align well with the results given by the Turn on Spot From Moving and Twist Till Orthogonal kinematics.

Other works have investigated factors such as the effect of lighting and room size [24], speech and gesture [34] and emotion [31] on proxemics zone sizes. These factors cannot be modelled with the kinematics approach only, hence form limitations of this work. Our models assume that thinking time is constant and do not take information gathering into account. They assume that Agent_1 knows the state of Agent_2 perfectly at all times. In reality, humans can see only in front of them, and need to take additional time to turn their eyes, head and/or body in order to see and understand the state of an agent behind or to the side of them. Such motions need to be initiated by some hint that an agent is there, such as an auditory cue. Following this, thinking time might then be a function of angle of approach, because humans detect objects faster if they are already looking in their direction than if they have to investigate a possible cue – such as a sound of footsteps or an engine – by turning their eyes, head or body to gather more information.

However, the best fits of our models to empirical data are obtained when thinking times are small, or zero. The zero thinking times could perhaps be explained by considering what human proxemic zones have evolved to do. Car stopping distances are calculated – and taught in driver training – to include the possibility of an unexpected or previously unseen event taking place which requires thinking time. However, for a human to even begin an interaction with another agent using proxemics, they must already have detected that agent. Thus it might be argued that the thinking time is zero given that an interaction has begun and the proxemic system has been brought into use.

More advanced biomechanics models could add details of leg and feet motions, for example each individual step creates a small local twist about the other foot on the ground which could be modeled. Walkers do not decelerate using friction as wheeled vehicles do, but they do have momentum which behaves in a similar way. The momentum may force them to take extra steps as they slow down and stop. Arm lengths and kinematics may also be important, as zones may be influenced by regions in which punches and grasps could be executed as well as whole-body collisions. Consideration of right-footedness versus left-footedness and the starting configuration of the pedestrian's feet and its bearing on which leg moves first in the escape zone might explain some of the lateral asymmetry that has been observed in some empirical cases [21, 37]. Factors including age and gender [38, 39], country [40] and social status [41] have been observed empirically to affect zone shapes and sizes, and pose challenges for future kinematic model extensions to explain.

Finding analytic solutions for the inner boundary of the social zone is surprisingly difficult, even for simple strategies. This suggests that humans and animals are unlikely to compute them explicitly, and must instead rely on learning them heuristically, either through long-term evolution, experience, or training.

Future work could run empirical experiments on human subjects to further test the model and obtain more accurate parameters. For example, a motion capture system could be used to track people's joints and movements and the data collected can be inserted into the models for validation. The models could be compared against each other to find which kinematics is the best fit to actual human motions such as Twist vs Turn On the Spot, possibly as a function of the environmental context; and the theoretical proxemic zones could be compared to empirically inferred ones using empirical methods from the previous studies.

In robotic navigation, understanding and manipulation of proxemic zones has been suggested in [4] as a potential solution to the freezing robot problem [1] in which mobile robots (including autonomous vehicles) programmed to be completely safe by yielding to pedestrians make no progress when pedestrians learn to continually push in front of them. The new, generative, understanding of the shapes and sizes of the personal zone introduced in the present paper could enable higher accuracy and more precise control in human-aware robot navigation systems.

When humans operate machinery for long periods – including driving vehicles and tele-operating industrial equipment – it is well known that they behave as if these machines are extensions of their bodies. We might thus expect them to learn and use new artificial proxemic zones which accurately reflect the speeds and escaping options of these machines. The stopping distances taught to learner drivers based on the '2-second rule' are an interesting example because they are taught and understood explicitly, before they become implicit feelings and reactions. Kinematic proxemics provides a way to understand how they become internalised and might suggest improved ways for teaching and learning them.

Funding This work has received funding from the EU H2020 project interACT: Designing cooperative interaction of automated vehicles with other road users in mixed traffic environments under grant agreement No 723395, and InnovateUK COVID19 Autonomous Delivery Vehicles (C19-ADVs) Project Reference 92211.

Data Availability No data was collected or analyzed as part of this work.

Code Availability The source code developed for this work is available on this zenodo repository: https://www.zenodo.org/records/17101548.

Declaration

Ethical Approval Not applicable.

Conflict of Interest The authors declare that they have no competing interests that are relevant to the content of this article.

References

1. Trautman P, Krause A (2010) Unfreezing the robot: navigation in dense, interacting crowds. In Proc. of the IEEE/RSJ international

conference on intelligent robots and systems (IROS), pp 797–803). https://doi.org/10.1109/IROS.2010.5654369
2. Fox CW, Camara F, Markkula G, Romano R, Madigan R, Merat N (2018) When should the chicken cross the road?: game theory for autonomous vehicle - human interactions. In VEHITS: 4th International conference on vehicle technology and intelligent transport systems. http://eprints.whiterose.ac.uk/127403/
3. Hall ET (1966) The hidden dimension., vol 609. Doubleday, Garden City, NY
4. Camara F, Fox C (2020) Space invaders: pedestrian proxemic utility functions and trust zones for autonomous vehicle interactions. Int J of Soc Robot. https://doi.org/10.1007/s12369-020-00717-x
5. Rios-Martinez J, Spalanzani A, Laugier C (2015) From proxemics theory to socially-aware navigation: a survey. Int J Soc Robot 7(2):137–153
6. Camara F, Fox C (2022) Extending quantitative proxemics and trust to HRI. In Proc. ofthe 31st Proc. of the IEEE International Conference on Robot & Human Interactive Communication (RO-MAN)
7. Lyubenov D (2011) Research of the stopping distance for different road conditions. Transp Probl 6:119–126
8. Camara F, Fox C A kinematic model generates non-circular human proxemics zones 37(24):1566–1575. https://doi.org/10.1080/01691864.2023.2263062
9. Koay KL, Syrdal D, Bormann R, Saunders J, Walters ML, Dautenhahn K (2017) Initial design, implementation and technical evaluation of a context-aware proxemics planner for a social robot. In Proceedings Social Robotics: 9th International Conference, ICSR 2017, vol 9. Springer, Tsukuba, Japan, 12–22). November 22–24, 2017
10. Aghaei M, Bustreo M, Wang Y, Bailo G, Morerio P, Del Bue A (2021) Single image human proxemics estimation for visual social distancing. In Proceedings of the IEEE/CVF winter Conference on Applications of Computer Vision, pp 2785–2795
11. Tatarian K, Chamoux M, Pandey AK, Chetouani M (2021) Robot gaze behavior and proxemics to coordinate conversational roles in group interactions. In 2021 30th IEEE International Conference on Robot & Human Interactive Communication (RO-MAN), pp 1297–1304). IEEE
12. Gao Y, Wallkötter S, Obaid M, Castellano G (2018) Investigating deep learning approaches for human-robot proxemics. In 2018 27th IEEE international symposium on Robot and Human Interactive Communication (RO-MAN), pp 1093–1098). IEEE
13. Satake S, Kanda T, Glas DF, Imai M, Ishiguro H, Hagita N (2009) How to approach humans? Strategies for social robots to initiate interaction. In Proceedings of the 4th ACM/IEEE International Conference on Human Robot Interaction, pp 109–116
14. Neggers MM, Cuijpers RH, Ruijten PA (2022) Ijsselsteijn, W.A.: determining shape and size of personal space of a human when passed by a robot. Int J Soc Robot 14(2):561–572
15. Duncan BA, Murphy (2012) R.R.: a preliminary model for comfortable approach distance based on environmental conditions and personal factors. In 2012 international conference on Collaboration Technologies and Systems (cts), IEEE, pp. 622–627
16. Hans A, Hans E (2015) Kinesics, haptics and proxemics: aspects of non-verbal communication. IOSR J Humanit And Soc Sci (iosr-Jhss) 20(2):47–52
17. Helbing D, Molnar P (1995) Social force model for pedestrian dynamics. Phys Rev E E 51(5):4282
18. Lehmann H, Rojik A, Hoffmann M (2020) Should a small robot have a small personal space? Investigating personal spatial zones and proxemic behavior in human-robot interaction. arXiv preprint arXiv:2009.01818
19. Jiménez MF, Scheidegger W, Mello RC, Bastos T, Frizera A (2022) Bringing proxemics to walker-assisted gait: using admittance control with spatial modulation to navigate in confined spaces. Pers ubiquitouscomput 26(6):1491–1509
20. Kirks T, Jost J, Finke J, Hoose S (2020) Modelling proxemics for human-technology-interaction in decentralized social-robot-systems. In Intelligent Human Systems Integration 2020: Proceedings of the 3rd International Conference on Intelligent Human Systems Integration (IHSI 2020): Integrating People and Intelligent Systems, Springer, Modena, Italy, 153–158). February 19–21, 2020
21. Gérin-Lajoie M, Richards CL, Fung J, McFadyen BJ (2008) Characteristics of personal space during obstacle circumvention in physical and virtual environments. Gait & posture 27(2):239–247
22. Hayduk LA (1981) The shape of personal space: an experimental investigation. Can J Behavioural Sci/Revue canadienne des Sci du comportement 13(1):87
23. Kosiński T, Obaid M, Woźniak PW, Fjeld M, Kucharski J (2016) A fuzzy data-based model for human-robot proxemics. In 2016 25th IEEE international symposium on robot and Human Interactive Communication (RO-MAN), pp 335–340). IEEE
24. Adams L, Zuckerman D (1991) The effect of lighting conditions on personal space requirements. J genpsychol 118(4):335–340
25. Horowitz MJ, Duff DF, Stratton LO (1964) Body-buffer zone: exploration of personal space. Arch Gen Psychiatry 11(6):651–656
26. Strube MJ, Werner C (1982) Interpersonal distance and personal space: a conceptual and methodological note. J nonverbalbehav 6:163–170
27. Kinzel AF (1970) Body-buffer zone in violent prisoners. Am J Psychiatry 127(1):59–64
28. Daza M, Barrios-Aranibar D, Diaz-Amado J, Cardinale Y, Vilasboas JA (2021) An approach of social navigation based on proxemics for crowded environments of humans and robots. Micromachines 12(2). https://doi.org/10.3390/mi12020193
29. Ginés Clavero J, Martín Rico F, Rodríguez-Lera FJ, Guerrero Hernández JM, Matellán Olivera V (2021) Defining adaptive proxemic zones for activity-aware navigation. In Advances in Physical Agents II: Proceedings of the 21st International Workshop of Physical Agents (WAF 2020), Alcalá de Henares). Springer, Madrid, Spain, 3–17). November 19–20, 2020
30. Kirby R, Simmons R, Forlizzi J (2009) Companion: a constraint-optimizing method for person-acceptable navigation. In RO-MAN 2009-The 18th IEEE International Symposium on Robot and Human Interactive Communication, pp 607–612). IEEE
31. Sousa RMD, Barrios-Aranibar D, Diaz- Amado J, Patiño-Escarcina RE, Trindade (2022) R.M.P.: a new approach for including social conventions into social robots navigation by using polygonal triangulation and group asymmetric gaussian functions. Sensors 22(12):4602
32. Barnaud M-L, Morgado N, Palluel- Germain R, Diard J, Spalanzani A (2014) Proxemics models for human-aware navigation in robotics: grounding interaction and personal space models in experimental data from psychology. In Proceedings of the 3rd IROS'2014 workshop "Assistance and Service Robotics in a Human Environment
33. Patompak P, Jeong S, Nilkhamhang I, Chong NY (2019) Learning proxemics for personalized human–robot social interaction. Int J Soc Robot 1–14
34. Mead R, Matarić MJ (2016) Perceptual models of human-robot proxemics. In: Experimental robotics: the 14th international symposium on experimental robotics. Springer, pp 261–276
35. Torta E, Cuijpers RH, Juola JF (2013) Design of a parametric model of personal space for robotic social navigation. Int J Soc Robot 5:357–365
36. Dubins LE (1957) On curves of minimal length with a constraint on average curvature, and with prescribed initial and terminal positions and tangents. Am JMath 79(3):497–516

37. Hase K, Stein R (1999) Turning strategies during human walking. J Educ Chang Neurophysiol 81(6):2914–2922
38. Petri HL, Huggins RG, Mills CJ, Barry LS (1974) Variables influencing the shape of personal space. In Proceedings of the Division of Personality and Society Psychology, vol 1 (1). pp 360–361
39. Oosterhout T, Visser A (2008) A visual method for robot proxemics measurements. In Proceedings of Metrics for Human-Robot Interaction: A Workshop at the Third ACM/IEEE International Conference on Human-Robot Interaction (HRI 2008). Citeseer, pp 61–68). Citeseer
40. Sorokowska A, Sorokowski P, Hilpert P, Cantarero K, Frackowiak T, Ahmadi K, Alghraibeh AM, Aryeetey R, Bertoni A, Bettache K et al. (2017) Preferred interpersonal distances: a global comparison. J Cross cultpsychol 48(4):577–592
41. Kiotas AJ (1990) The relation of social status and gender to static and dynamic proxemic variables. University of Delaware